

Unconventional Behavior of $\text{YBa}_2\text{Cu}_3\text{O}_{7-\delta}$ Grain Boundary Tunnel Junctions between 4.2 K and 300 K

C. W. Schneider, S. Hembacher, G. Hammerl, R. Held, A. Schmehl, A. Weber,
T. Kopp, and J. Mannhart

*Experimentalphysik VI, Center for Electronic Correlations and Magnetism, Institute of Physics,
Augsburg University, D-86135 Augsburg, Germany*

(May 22, 2019)

Abstract

Current-induced dissipation in $\text{YBa}_2\text{Cu}_3\text{O}_{7-\delta}$ grain boundary tunnel junctions has been measured between 4.2 K and 300 K. The resistance of (100)/(110) junctions decreases linearly by a factor of four with temperature increasing from 100 K to 300 K. At the superconducting transition temperature T_c the grain boundary resistance of the normal state and of the superconducting state extrapolate to the same value. The transition into the superconducting state is found not to affect the dissipation in the junctions at T_c .

74.20.Rp, 74.50.+r, 74.76.Bz, 85.25.Cp

Soon after the discovery of superconductivity in $\text{La}_{2-x}\text{Ba}_x\text{CuO}_4$ [1], it was realized that the high- T_c superconductors are characterized by extraordinary properties of the non-superconducting state, in addition to the remarkable superconducting behavior exemplified by their high transition temperature T_c and the predominant $d_{x^2-y^2}$ -wave pairing symmetry. The most prominent, still unresolved, unconventional normal state properties are the linear temperature dependence of the in-plane resistivity of the optimally doped compounds [2], spin and charge inhomogeneities [3], and the pseudogap present in the underdoped regime [4].

The complex electronic behavior of the high- T_c cuprates is also reflected in the properties of their interfaces. In the superconducting state, for example, large-angle grain boundaries act as excellent tunnelling barriers [5]. This behavior is unknown from conventional superconductors. Several mechanisms responsible for the electronic transport properties of grain boundaries for temperatures $T < T_c$ have been identified, such as the $d_{x^2-y^2}$ dominated order parameter symmetry, structural effects and space charge layers [5]. In fact, grain boundaries operated below T_c have been used to clarify important properties of the high- T_c cuprates, such as the existence of Cooper pairs [6] or the unconventional order parameter symmetry [7].

As for the temperature regime below T_c , we expect valuable and possibly surprising information on the interfaces of the cuprates or even on the bulk material itself to be contained in the tunneling characteristics of the boundaries measured in the temperature range above T_c . However, little data are available for this temperature regime [5, 8]. The lack of data arises from the difficulty to measure the grain boundary current-voltage ($I(V_{\text{gb}})$) characteristics free of voltages produced by the intragrain parts of the bridge that are needed to contact the boundary. The grains are resistive for $T > T_c$. Using appropriate techniques to subtract these unwanted voltages, we report here on measurements of the resistance and the current-voltage characteristics of well defined $\text{YBa}_2\text{Cu}_3\text{O}_{7-\delta}$ grain boundaries between 4.2 K and 300 K.

The experiments were performed with grain boundaries fabricated with the bicrystal technology [9]. The epitaxial films were deposited by pulsed laser deposition from $\text{YBa}_2\text{Cu}_3\text{O}_{7-\delta}$ targets onto [001]-tilt SrTiO_3 -bicrystals containing symmetric and (100)/(110)-asymmetric 45° grain boundaries, specified to within 1°. The deposition was carried out at a heater temperature of 760°C in an oxygen pressure of $P = 0.25$ mbar. After deposition, the samples were cooled during two hours at $P = 400$ mbar. Special care was taken to ensure the homogeneity of the samples. The film thicknesses were adjusted to a typical value of 40–50 nm, measured by scanning force microscopy. These measurements revealed variations of less than 10 % in the thickness of the $5 \times 10 \text{ mm}^2$ large films. T_c varied less than 0.5 K on a wafer. Gold contacts were structured photolithographically before the $\text{YBa}_2\text{Cu}_3\text{O}_{7-\delta}$ films were patterned by etching in a H_3PO_4 solution, or dry etching using an Ar ion-beam. The bridges measured in four-point configurations had widths and lengths between the voltage probes of $\approx 2.5 \mu\text{m}$ and $30 \mu\text{m}$, respectively (see Fig. 1), their T_c varied less than 200 mK. Several samples were patterned in addition into Wheatstone-bridge configurations, of which each arm consists of a meander line containing 23 straight sections with widths of $\approx 6 \mu\text{m}$. Two of the meander lines were patterned such that each of the 23 sections crosses the boundary once.

The measurements were conducted in an electrically and magnetically shielded room. Below T_c , the technique to precisely measure the grain boundary resistance R_{gb} is based on

measuring the $I(V_{\text{gb}})$ characteristic of the Josephson junction, while applying a microwave field that is sufficiently large to suppress the Josephson current. For this, we used low frequency microwaves (< 10 GHz) to avoid inaccuracies resulting from the otherwise non-negligible height of the microwave-induced Shapiro steps.

For $T > T_c$ the transport properties of the interfaces cannot be measured with a straightforward four-point technique. This is because the voltage V_{meas} generated by a bridge straddling the boundary is composed of the grain boundary voltage V_{gb} and of the voltages $V_{\text{g}1}$ and $V_{\text{g}2}$ caused by the parts of the resistive grains located inside the bridge. This problem can be solved by subtracting from V_{meas} the grain contributions $V_{\text{g}1}$ and $V_{\text{g}2}$. For this, $2V_{\text{g}1}$ and $2V_{\text{g}2}$ are obtained by approximating them with the voltages $V_{\text{g}1}^*$ and $V_{\text{g}2}^*$ generated by independent intragrain bridges measured simultaneously. Not surprisingly, test measurements with samples containing a number of intragrain bridges revealed variations of $V_{\text{g}1}^*$ and $V_{\text{g}2}^*$ of several percent as a function of the bridge location. Therefore, we placed the intragrain bridges as close as possible to the grain boundary bridge (see Fig. 1). The desired measurement accuracy also determined the optimum size of the bridges. On the one hand the bridges were patterned to be as small as possible so that they could be located close to the grain boundary. On the other hand, their size was chosen to be large enough for the patterning-induced scatter of the bridge aspect ratios to be insignificant. In samples optimized this way, the voltages across the two bridges $V_{\text{g}1}^*$ and $V_{\text{g}2}^*$ were identical to within 1% at 100 K and 0.3% for $T > 200$ K, so that the grain boundary voltage equals with the same accuracy

$$V_{\text{gb}} \approx V_{\text{meas}} - (V_{\text{g}1}^* + V_{\text{g}2}^*)/2 . \quad (1)$$

As introduced by Mathur *et al.* [10] for studies of $\text{La}_{1-x}\text{Ca}_x\text{MnO}_3$ bicrystals, and similar to the work described in Ref. [8], we also patterned several samples into Wheatstone-bridges. This approach has the advantage that the voltage generated by the large meander structure is huge and that already during the measurement $V_{\text{g}1}^*$ and $V_{\text{g}2}^*$ are subtracted from V_{meas} . Having performed measurements with such bridges, we checked their balance by photolithographically cutting the Wheatstone-configurations, to measure the resistances of the four meander lines individually. Because these studies revealed temperature-dependent balancing errors of 1–10 %, we preferred the three-bridge approach for measurements of the temperature dependence of the grain boundary resistance ($R_{\text{gb}}(T)$), and Wheatstone-bridges when a large signal was required, as was the case for some studies of $I(V)$ characteristics.

To gain insight into the electronic transport mechanisms, we measured the $I(V)$ characteristics between 4.2 K and 300 K by using Wheatstone-bridges. The upper limit of the applied voltages is given by the onset of heating, signalled by a resistance decrease. For $T > T_c$ the characteristics are non-linear on this large voltage scale, in particular below 150 K (see Fig. 2). Analyzing the non-linearity, we first note that the microstructure of the grain boundaries is inhomogeneous down to the unit cell level [11, 12]. The $I(V)$ curves are therefore generated by large numbers of microstructurally different channels connected in parallel and they have to be analyzed with caution. This in mind, we note that the behavior of the averaged junctions is consistent with the one of a back-to-back Schottky contact as predicted by the band bending model [13]. If tentatively described by a Simmons-fit [14], the averaged $I(V)$ characteristics correspond to heights and widths of the hypothetical effective junction barriers of ≈ 100 meV and 1–2 nm. Thus, these data suggest unusually

small barrier heights. They are, in particular, much smaller than the energy scale of grain boundary built-in potentials measured by electron-holography of ≈ 2 eV [15]. As considered by Miller and Freericks [16], if present, electronic correlations in the barriers modify the local transport. Consequently, it is proposed that electronic correlations, enhancing for example electronic inhomogeneities, affect the barrier properties besides the more conventional mechanisms.

At small voltages, $V_{\text{gb}} \lesssim 10$ mV, the non-linearity of the $I(V)$ curves is insignificant, and they are characterized by their ohmic resistance, which can be obtained by selecting an appropriate voltage (V_{cr}) or current (I_{cr}) criterion $V_{\text{cr}} = I_{\text{cr}} \times R_{\text{gb}} < 10$ mV. For $T < T_c$, due to the microwave irradiation, the $I(V)$ characteristics are linear, too, even over a larger voltage range. The only exception is given by 45° boundaries at $T < 40$ K, which will be discussed below. Applying the three-bridge technique, we were therefore able to deduce the $R_{\text{gb}}(T)$ dependence of a given grain boundary by measuring in one temperature sweep from 4.2 K to 300 K just one boundary bridge plus the two intragrain reference bridges, using one voltage or current criterion for all temperatures, typically $I_{\text{cr}} = 100$ μ A. As for such a voltage bias the dissipated power is always smaller than 1 μ W, all heating effects are negligible over the whole temperature regime.

The $R(T)$ -dependence of a 45° symmetric grain boundary measured this way is presented in Fig. 3. It is noted that the resistance-area product $R_{\text{gb}}A$ (77 K) $\approx 1 \times 10^{-8}$ Ωcm^2 compares well with literature values [5]. Three remarkable features are displayed by the temperature dependence of the resistance. First, the resistance of 45° boundaries reaches a maximum at ≈ 30 K (see also Fig. 4). This maximum is not displayed by symmetric 24° boundaries measured as reference samples. Second, between 100 K and 300 K the resistance decreases with increasing temperature by a factor of four. The temperature dependence is hereby stunningly linear, with a barely noticeable positive curvature (see upper inset). This is in striking contrast to the linear resistance increase of the adjacent $\text{YBa}_2\text{Cu}_3\text{O}_{7-\delta}$ grains (see lower inset). Third, around T_c the resistance develops a distinct peak structure. This peak, which is not associated with the microwave irradiation, was found to vary from sample to sample, and within one sample over a time scale of weeks. Except for this peak, the grain boundary resistance of the normal state and of the superconducting state extrapolate within the measurement accuracy of $\approx 2\%$ to the same value $R_{\text{gb}}(T_c) = 10.7\Omega$. This temperature dependence is characteristic for all samples we have studied, with the exception of several samples that displayed at T_c a resistance step of $\lesssim 5\%$. As this step was found to be not reproducible from sample to sample and to increase for a given sample on a time scale of weeks, we do not consider it to be an intrinsic property of the grain boundaries, but to be an artifact resulting from chemical reactions or diffusion.

In the following, we will discuss the three features and their implications for the understanding of the interfaces, beginning with the low temperature regime.

At low temperatures, the resistance of 45° grain boundaries changes non-monotonically with T , and, as mentioned above, even depends on the value of the tunneling current. For a small bias current a maximum at ≈ 30 K is developed, which shifts to lower temperatures at larger bias (see Fig. 4). This maximum and its current bias dependence are consistent with the formation of a zero-bias anomaly by the faceted 45° junctions. At small bias currents V_{gb} is of the order 1 mV, and therefore sufficiently small to probe the temperature dependent shape of the zero-bias conductance peak in the superconducting energy gap. This zero-bias

conductance peak is usually presumed to arise from Andreev bound states generated by the $d_{x^2-y^2}$ order parameter symmetry of $\text{YBa}_2\text{Cu}_3\text{O}_{7-\delta}$ [19], which in this case manifests itself even in the $R_{\text{gb}}(T)$ characteristic.

For $T > T_c$, $R_{\text{gb}}(T)$ decreases linearly. There are three different mechanisms which have to be considered to contribute to this behavior. The first is thermally activated hopping over the barrier, as suggested by the analysis of the $I(V)$ curves which proposes microscopic areas at the boundaries to exist with barrier heights below 100 meV. Second, with increasing temperature, thermal smearing of the Fermi-edge opens direct and indirect tunneling channels [20], thereby reducing R_{gb} . Third, due to the possibly temperature-dependent electrostatic screening length $\lambda_{\text{el}}(T)$ and built-in potential $V_{\text{bi}}(T)$ generated by charges located at the boundary, it has to be expected that the height and width of the tunneling barrier decrease with increasing temperature [8,17]. But also the analysis of the $R_{\text{gb}}(T)$ -dependence is complicated by the inhomogeneous microstructure of the boundaries. The curves reflect the average of many microscopic channels, of which neither the resistances nor the temperature dependencies are known, preventing at present a more detailed analysis of the intriguing question whether the linear decrease of the tunneling resistance with temperature is the fingerprint of one dominating mechanism.

The third feature of the $R_{\text{gb}}(T)$ -dependence, the peak structure at T_c , provides evidence that at T_c the resistance of the grain boundary bridge is much larger than the resistance of the intragrain-bridges. The observed height of the peak shown in Fig. 3 is consistent with a T_c difference of the bridges of 150 mK. The shape of the peak may be influenced by the differences in the fluctuations of the intragrain bridges and the one containing the tunnel junction. Unfortunately we cannot extract data on this effect from the peak, as the spatial distribution of T_c is unknown.

The grain boundary resistance values above and below T_c extrapolate to the same value at the transition temperature. The transition into the superconducting state is therefore found not to affect the dissipation in the junctions at T_c . This observation cannot be reconciled with the predictions for surface charging effects in the hole superconductivity scenario introduced by Hirsch and coworkers [21]. In this scenario, charges are separated in the superconducting state in the vicinity of a grain boundary, but not above T_c . This charge separation is expected to change the electronic properties of the interfaces when passing T_c [22]. The grain boundary data do not show this effect.

In summary, the resistance of 45° [001]-tilt $\text{YBa}_2\text{Cu}_3\text{O}_{7-\delta}$ grain boundary junctions has been measured and found to be linearly decreasing with increasing temperature for $T > T_c$. In the vicinity of T_c the grain boundary resistance and thus the dissipation is indistinguishable for $T < T_c$ and $T > T_c$, in contradiction to predictions of the theory of hole superconductivity. The non-linear current-voltage characteristics measured between 4.2 K and 300 K predict an effective barrier height of ≈ 0.1 eV and an effective barrier width of $\approx 1\text{--}2$ nm.

The authors gratefully acknowledge helpful discussions with Y. Barash, H. Bielefeldt, M. Blamire, U. Eckern, P.J. Hirschfeld, C. Laschinger, J. Ransley, D.G. Schlom, and M. Siegel. This work was supported by the Deutsche Forschungsgemeinschaft through the SFB 484 and by the BMBF via project 13N6918A.

REFERENCES

- [1] J. G. Bednorz and K. A. Müller, Z. Phys. B **64**, 189 (1986).
- [2] S.W. Tozer *et al.*, Phys. Rev. Lett. **59**, 1768 (1987).
- [3] J. Orenstein and A. J. Millis, Science **288**, 468 (2000).
- [4] T. Timusk and B. Statt, Rep. Prog. Phys. **62**, 61 (1999).
- [5] H. Hilgenkamp and J. Mannhart, Rev. Mod. Phys. **74**, 485 (2002).
- [6] C. E. Gough *et al.*, Nature **326**, 855 (1987).
- [7] C. C. Tsuei and J. R. Kirtley, Rev. Mod. Phys. **72**, 969 (2000).
- [8] J. H. T. Ransley *et al.*, unpublished.
- [9] D. Dimos *et al.*, Phys. Rev. Lett. **61**, 219 (1988).
- [10] N. D. Mathur *et al.*, Nature **387**, 266 (1997).
- [11] C. Traeholt *et al.*, Physica C **230**, 425 (1994).
- [12] J. Mannhart *et al.*, Phys. Rev. Lett. **77**, 2782 (1996).
- [13] J. Mannhart and H. Hilgenkamp, Mat. Sci. Eng. **B56**, 77 (1998).
- [14] J. G. Simmons, J. Appl. Phys. **34**, 1828 (1963).
- [15] M. A. Schofield *et al.*, Phys. Rev. B **67**, 224512 (2003).
- [16] P. Miller and J. K. Freericks, Journ. of Phys. **13**, 3187 (2001).
- [17] H. Hilgenkamp and J. Mannhart, Appl. Phys. Lett. **73**, 265 (1998).
- [18] A. Gurevich and E. A. Pashitskii, Phys. Rev. B **57**, 13878 (1998); err: **63**, 139901 (2001).
- [19] C.-R. Hu, Phys. Rev. Lett. **72**, 1526 (1994).
- [20] L. I. Glazman and K. A. Mateev, Sov. Phys. JETP **67**, 1276 (1988); err: **49**, 659 (1989).
- [21] J. Hirsch and F. Marsiglio, Phys. Rev. B **39**, 11515 (1989).
- [22] J. Hirsch, Phys. Lett. A **281**, 44 (2001).

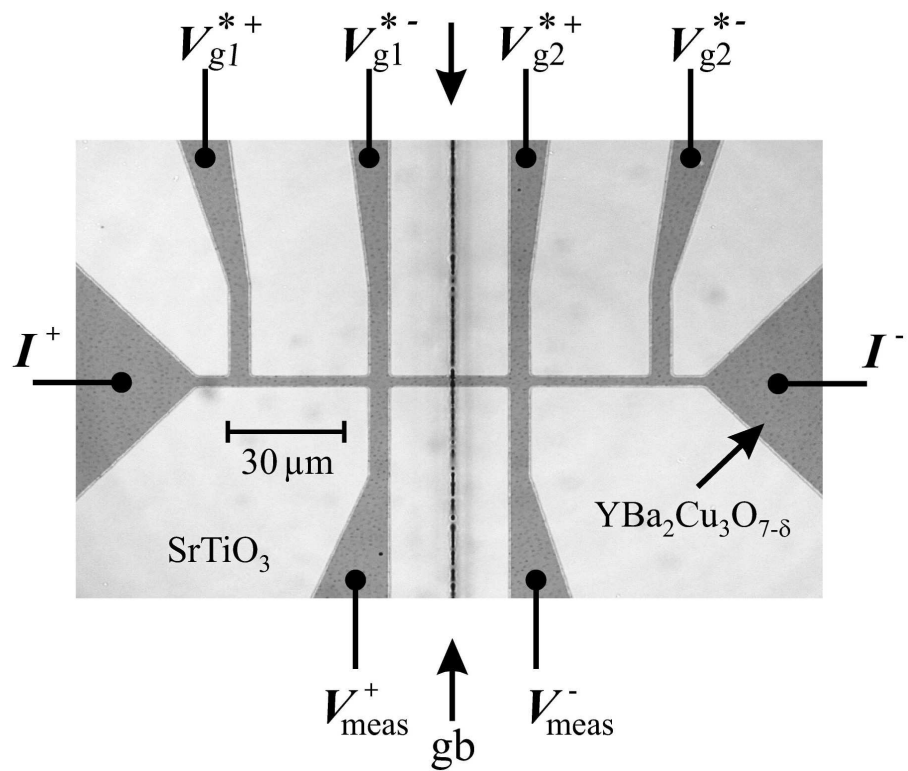
FIGURES

FIG. 1. Optical micrograph of a three-bridge sample used to measure R_{gb} . The position of the symmetric 45° grain boundary (gb) is indicated by the arrows.

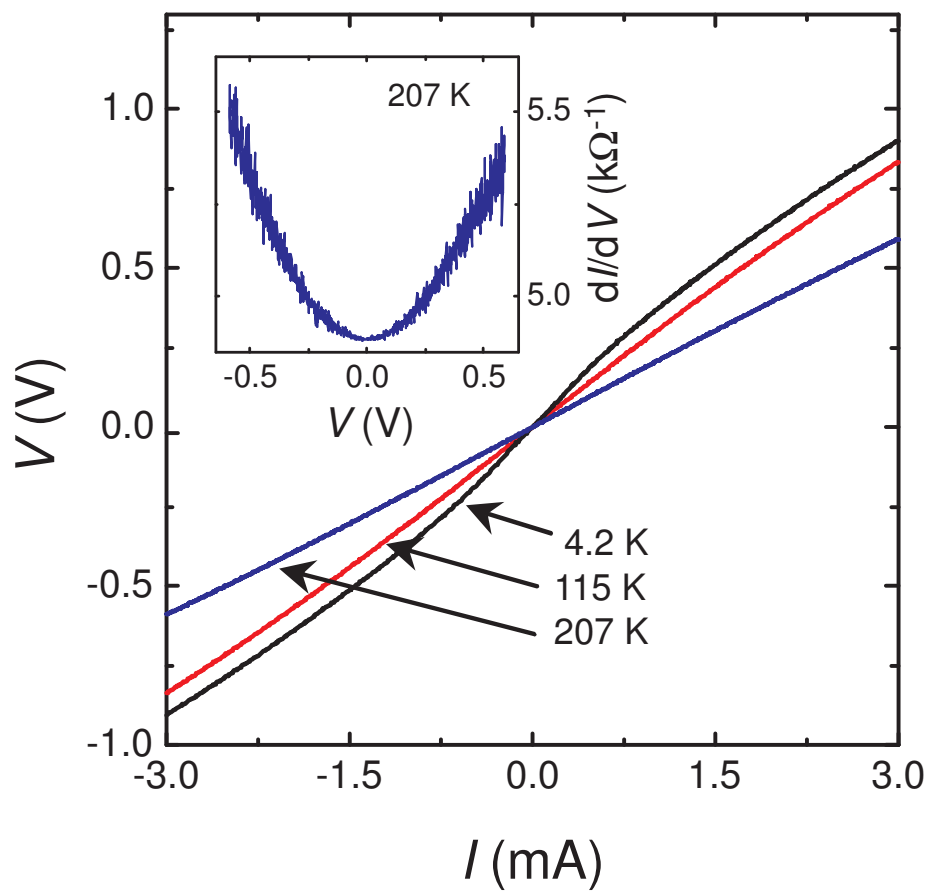
FIG. 2. Current-voltage characteristics of a Wheatstone-bridge containing 23 junctions with a 45° asymmetric boundary in a 50 nm thick $\text{YBa}_2\text{Cu}_3\text{O}_{7-\delta}$ film. The voltage V corresponds to the voltage across all junctions, $V = 23 \times V_{gb}$, the current I is twice the current flowing through one meander line.

FIG. 3. Measured temperature dependence of the resistance of a 45° symmetric grain boundary in a 40 nm thick $\text{YBa}_2\text{Cu}_3\text{O}_{7-\delta}$ film ($I_{cr} = 100 \mu\text{A}$). The peak reaches a maximum of 25Ω at 88.3 K. The insets show $dR/dT(T)$ for the grain boundary and the corresponding $R(T)$ curve of one grain located next to the boundary.

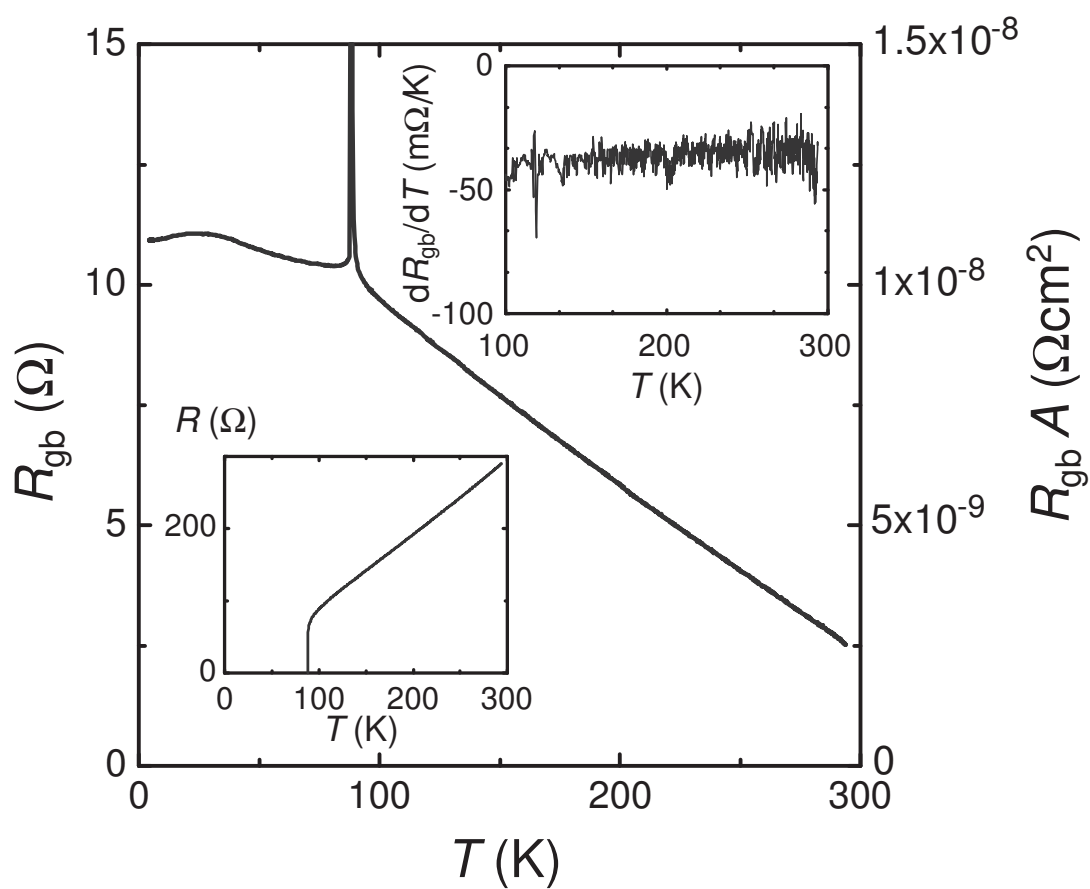
FIG. 4. Temperature dependence of the resistance of a 45° symmetric grain boundary in a 40 nm thick $\text{YBa}_2\text{Cu}_3\text{O}_{7-\delta}$ film measured in the three-bridge configuration. The inset shows the temperature dependent resistance of a 45° asymmetric grain boundary in a 50 nm thick film measured in a Wheatstone-bridge configuration.



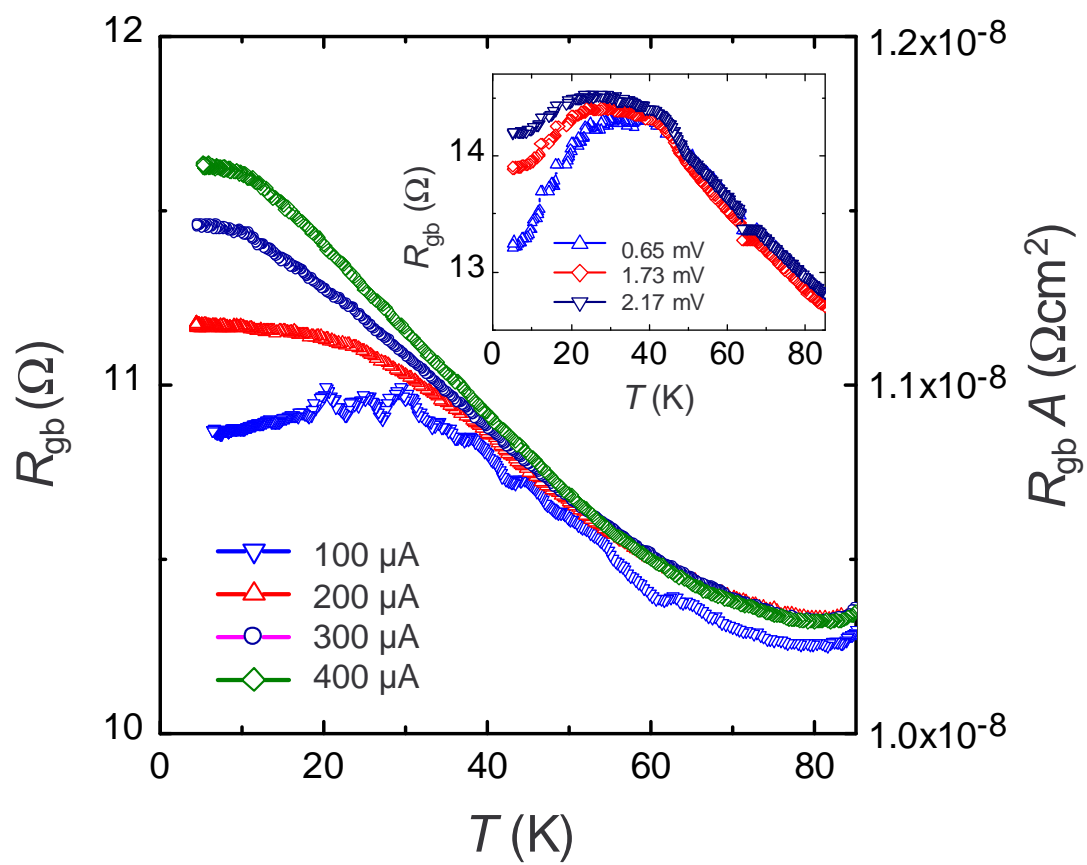
Schneider et al., Figure 1



Schneider *et al.*, Figure 2



Schneider *et al.*, Figure 3



Schneider *et al.*, Figure 4